NANO LETTERS

pubs.acs.org/NanoLett

Letter

Enhanced Nanoscale Ge Concentration Oscillations in Si/SiGe Quantum Well through Controlled Segregation

Kevin-P. Gradwohl,* Lukas Cvitkovich, Chen-Hsun Lu, Sebastian Koelling, Maximilian Oezkent, Yujia Liu, Dominic Waldhör, Tibor Grasser, Yann-Michel Niquet, Martin Albrecht, Carsten Richter, Oussama Moutanabbir, and Jens Martin

Cite This: *Nano Lett.* 2025, 25, 4204–4210

Read Online

ACCESS | Metrics & More | Article Recommendations | Supporting Information

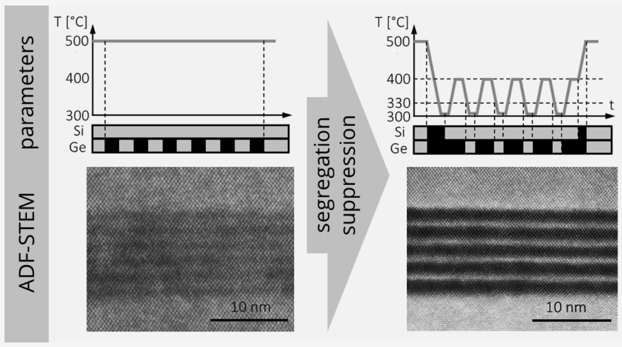

ABSTRACT: The integration of electron spin qubits on Si/SiGe heterostructures requires precise control of valley splitting associated with conduction band degeneracy. This can be achieved by introducing nanoscale oscillating Ge concentration profiles, known as Wiggle Wells. However, the intermixing and segregation of Ge during growth have hindered their realization. We report the growth of Si/SiGe heterostructures with clear nanoscale composition modulation within the quantum well using molecular beam epitaxy. By oscillation of the growth temperature, Ge segregation is suppressed, achieving a Ge concentration modulation of 30%/nm, an order of magnitude higher than prior results. Tight-binding simulations suggest that Wiggle Well heterostructures with sharp compositional transitions significantly enhance valley splitting, yielding average values exceeding 200 μeV, with energy levels well separated from 0 μeV. Hence, Wiggle Wells are a promising approach for Si-based electronic qubits.

KEYWORDS: *silicon, germanium, molecular beam epitaxy, segregation, spin qubit, valley splitting*

Electron spin qubits in gate-defined silicon quantum dots based on SiGe heterostructures are a promising and fast-developing technology for quantum computing.[1−5] These heterostructures typically consist of strained Si quantum well layers coherently grown on relaxed $Si_{0.7}Ge_{0.3}$, where the strain partially lifts the conduction band valley degeneracy. Lifting the remaining 2-fold degeneracy in a reliable way poses a challenge currently limiting the scalability of Si-based spin-qubits.[6−8] Hence, leveraging advantages of the elaborated fabrication techniques used in the silicon industry for quantum applications and consequently the reliable integration of a large number of qubits in this material platform first requires a technology that allows for a large and controllable valley splitting E_v of the conduction band valley degeneracy to be achieved through material design.[9]

Several approaches have been proposed and explored in the past, including SiGe heterostructures with atomically flat interfaces, atomic fluctuations due to Ge alloying, and modifications of the quantum well barriers.[10,11] However, most recently, a nanoscale oscillating Ge concentration in the quantum well, a so-called wiggle quantum well (WQW), was proposed as a way to achieve a large and tunable E_v.[12] Hereby, a Ge oscillation with a wave vector q is chosen to couple the conduction-band valleys within or between Brillouin zones. For ideal coupling, this translates to real space oscillations with $q \approx 20$ nm^{-1} (periodicity $P = 0.32$ nm) and $q \approx 3.5$ nm^{-1} ($P = 1.8$ nm), respectively. E_v can be further enhanced by applying shear strain to the WQW (e.g., by fabricating special trenches via lithography).[13] While adding Ge atoms to the quantum well layer comes with potential trade-offs such as an additional disorder, as was shown by mobility measurements,[12] WQWs promise enhancement of E_v with a minimal amount of Ge in the quantum well. Furthermore, this nanoscale Ge oscillation can also be utilized to enhance spin−orbit coupling, opening the possibility of utilizing intrinsic spin-obit coupling for fast gate operations.[14]

In the original proposal of WQW heterostructures,[12] quantum dot devices were demonstrated and their respective valley splitting was determined by pulsed-gate spectroscopy. Even though the valley splitting was large and tunable, between 54 and 239 μeV, their simulations indicated that valley splitting is dominated by random Ge concentration fluctuations

Received: October 25, 2024
Revised: January 6, 2025
Accepted: January 6, 2025
Published: March 4, 2025

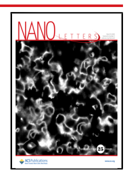

https://doi.org/10.1021/acs.nanolett.4c05326
Nano Lett. 2025, 25, 4204−4210

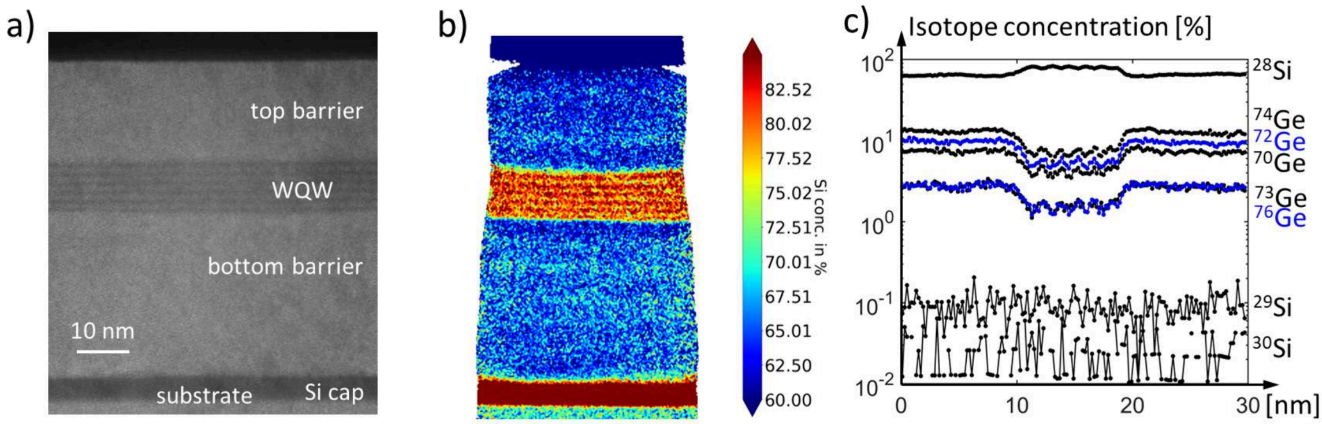

Figure 1. (a) shows an ADF-STEM image of a WQW heterostructure grown on a strain-relaxed SiGe buffer substrate with a 5 nm Si cap at a growth temperature of 500 °C; the respective APT image is shown in (b). (c) shows the Si and Ge isotope concentration throughout the WQW.

associated with SiGe random-alloy disorder and not by the distinct Ge concentration oscillations. This moderate valley splitting (VS) can be ascribed to the limited Ge concentration gradient, reducing the modulation amplitude in their heterostructures grown by chemical vapor deposition (CVD) at 600 °C growth temperature.[15] At these elevated temperatures, growth is dominated by Ge segregation, which ultimately limits spatial concentration gradients independent of absolute Ge concentration.[16]

Hence, further material development is required to realize pronounced nanoscale Ge concentration oscillations. Another relevant aspect is the impact of the postgrowth device fabrication processes involving ion implantation and thermal annealing on the Ge profile in the well, which is beyond the scope of this work that focuses on the material growth challenges.

Here, we demonstrate and investigate the potential of growing SiGe WQW heterostructures by molecular beam epitaxy (MBE) on strain-relaxed SiGe buffers. MBE allows for growth at lower temperatures utilizing ultrahigh vacuum (UHV) yielding ultimately higher compositional control and steeper concentration gradients.[17] We investigated the materials challenges to realize sharp and substantial Ge-profiles in WQWs, in particular approaches to suppress Ge segregation in MBE, while maintaining high-quality crystalline material as well as the demonstration of the robustness of WQW-induced VS against statistical fluctuations by numerical means. The focus lies hereby on the material development of quantum well layers with Ge concentration oscillations with 4 and 5 periods. This corresponds to wavelengths of around 1.8 and 2.3 nm for a typical quantum well layer thickness of 10 nm, which is still below the critical thickness for relaxation.

Tight-binding (TB) simulations based on the actually achieved material contrast of MBE-grown material reveal robust values for the valley splitting energies E_v above 200 μeV, significantly higher compared to the estimated valley splitting of random Ge alloy contributions alone and with an energy distribution which is clearly offset from 0 μeV.

We start our discussion by considering a $Si_{0.7}Ge_{0.3}$/Si/$Si_{0.7}Ge_{0.3}$ heterostructure (target composition) grown at a constant growth temperature of 500 °C with P = 1.8 nm as shown in the scanning transmission electron microscopy (STEM) image in Figure 1a. Hereby, 500 °C is the optimal temperature to grow $Si_{0.7}Ge_{0.3}$ and Si in molecular beam epitaxy, allowing for a growth interrupt-free process.[6] Further experiments at different growth conditions are presented in Supporting Information S1.

A distinct Ge concentration oscillation, apparently more pronounced than the originally reported WQW heterostructures grown by CVD at 600 °C, can be identified.[12] The atom probe tomography (APT) data in Figure 1b reveal a deviation from the targeted composition of the barriers (38% Ge instead of 30% Ge). This increase is Ge content has no impact on the conclusions drawn from these investigations. Furthermore, the APT data reveal that the WQW exhibits a Ge modulation of only a few atomic % around a medium value of 20% Ge, even though from the respective evaporation rates of Ge and Si one would naively expect a Ge concentration modulation of at least 38%.

This can be explained by the growth-related phenomenon referred to as Ge segregation.[18,19] Hereby, the formation of an energetically favorable Ge adlayer results in site exchange between subsurface Ge and surface Si atoms, blurring the interfaces. For growth temperatures of 380 °C and above, concentration slopes limited to 3%/nm independent of concentration and growth temperature were reported.[20] The segregation can be reduced by lowering the growth temperature or the use of surfactants (e.g., Bi, Sb, Ga) during epitaxy.[20,21] However, surfactants are ruled out here due to the high additional quality requirements for spin qubit operation (undoped, without charge traps, and nuclear spin-free).

Figure 1c shows the isotope concentration in the WQW. Hereby, natural Ge and an isotopically enriched ^{28}Si source have been utilized.[22] Hence, while the Ge isotope concentrations of ^{70}Ge, ^{72}Ge, ^{73}Ge, ^{74}Ge, and ^{76}Ge are in agreement with the natural isotope abundance, the heterostructure exhibits a sufficiently low concentration of ^{29}Si and ^{30}Si of 10^{-1} % and 10^{-2} %, respectively. Ultimately, qubits based on Si/SiGe heterostructures have to leverage the possibility of being grown nuclear spin-free, which, in particular, means free of ^{29}Si and ^{73}Ge. In the future, the use of nuclear spin-free Ge source material and experimental demonstration of devices is planned but is currently beyond the scope of this work.

The contrast in annular dark-field (ADF) imaging by STEM depends on the atomic number Z of the investigated material and consequently embodies a powerful technique to investigate concentration modulations with a high spatial

https://doi.org/10.1021/acs.nanolett.4c05326
Nano Lett. 2025, 25, 4204−4210

resolution. It has been reported that the ADF contrast Q_{ADF} is a power law in form of[23]

$$Q_{ADF} \propto \sum_i Z_i^n \quad (1)$$

where Z_i is the atomic number of the ith atom in the unit cell and n is a parameter typically between 1 and 2. Substituting this sum with an average atomic number of $(1 - x)Z_{Si} + x{\cdot}Z_{Ge}$ of a perfect $Si_{1-x}Ge_x$ random alloy by using and applying the logarithm on both sides allows us to rewrite eq 1 as

$$\log(Q_{ADF}) \propto n{\cdot}\log(\Delta Z{\cdot}x + Z_{Si}) \quad (2)$$

Hence, the Ge concentration x can be calculated from the ADF-STEM contrast for a given measurement condition, provided that n is determined with a reference measurement. Here, this is achieved by comparison to APT data, as can be seen in Figure 2. Note that the data related to the Si cap interfaces of the substrate were removed, as well as the very surface of the heterostructure. The data corresponding to the barrier, WQW, and Si cap are labeled in Figure 2a. The data points between the barriers and the WQW correspond to the interfaces at the boundary of the WQW. The slope of a least-squares fit to the power law described in eqs 1 and 2 is indicated by the red dotted line and results in the exponent n = 1.36. We will exploit this model to quantify the Ge content from STEM images of the heterostructures discussed below.

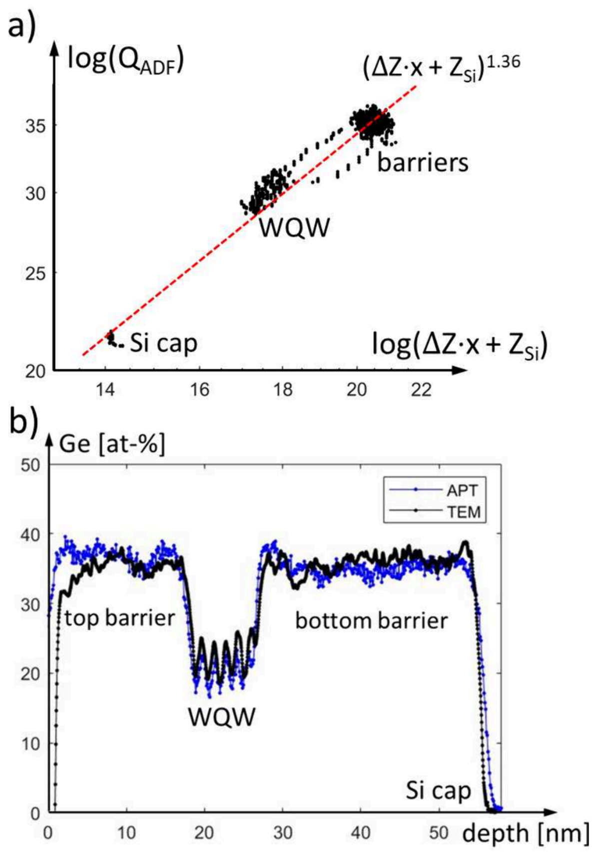

Figure 2. (a) Display of the recorded intensity Q_{ADF} of the ADF-STEM measurements and the Ge concentration x, weighted by the difference in atomic numbers ΔZ between Z_{Si} and Z_{Ge} in black. The red dotted line shows the least-squares fit of a power law with n = 1.36. (b) Compositional data from APT compared with the calculated composition from the STEM measurement using the above model.

The realization of a WQW with enhanced valley splitting requires pronounced Ge concentration oscillations. Hereby, it is clear that controlling Ge segregation is key. One way to suppress Ge segregation is a reduction of the growth temperature.

It was shown that segregation is effectively suppressed by growing the first Ge-rich layers on Si-rich SiGe below 330 °C and the Si-rich layers on Ge-rich SiGe at 300 °C.[24] However, below 400 °C Si growth with smooth surfaces and large terrace widths cannot be accomplished.[25] Consequently, for an ideal WQW growth, one has to oscillate the growth temperature, realizing lower temperatures at the interfaces to suppress segregation and higher temperatures in between to achieve smooth surfaces.

We have realized SiGe growth with such a temperature variation. In Figure 3, we compare a sample grown at constant growth temperature with a heterostructure grown at optimized temperatures at each step of the heterostructure. The required oscillating growth temperature as a function of time together with the Si and Ge shutter configurations is depicted in Figure 3d.

The fast Ge oscillation in the proposed WQW heterostructures makes the growth a nontrivial task and requires extremely low growth rates due to the limited heating/cooling ramps that can be realized in MBE, which in turn requires controlled growth conditions (e.g., vacuum conditions). Here, evaporation rates of 0.001 nm/s (around 0.1 monolayer/min) were employed for the heterostructure shown in Figure 3e.

The comparison between ADF-STEM images of the two heterostructures displays a striking difference in the Z-contrast and consequently in the Ge concentration modulation. The respective Ge concentration profile along the WQW calculated from the STEM images according to the model described in the previous section, is depicted in Figure 3c,f. This approach is justified since the measurement conditions were identical (see the experimental section in the Supporting Information for greater detail). The suppression of the Ge segregation at reduced growth temperatures allows for much lower average Ge concentrations in the WQW. It is not unambiguously clear to which degree the remaining Ge concentration in the valleys of the WQW is real or an artifact resulting from the TEM contrast interpretation. From the Ge concentration profiles the maximal slopes in the WQWs can be quantified to be 10%/nm for a constant growth temperature of 500 °C and up to 30%/nm for oscillating growth temperature. In particular the latter demonstrates the efficiency in suppressing Ge-segregation, by reduced temperature growth.

The experimentally derived concentration profiles are used as inputs to tight-binding simulations to determine realistic heterostructure designs and their respective predicted valley splitting.

The expected valley splitting of a variety of possible WQW heterostructures was determined by tight-binding simulations, taking into consideration the obtained sharpness in compositional transitions (a maximum of 30%/nm). The sp3d5s* Hamiltonian is constructed based on parameters from refs 26 and 27 and comparable to the models used in recent modeling studies.[12,28] A representative simulation cell of a WQW heterostructure is shown in Figure 4a. Ge oscillations with a peak concentration $\hat{n}_{Ge}$ of 20% and 10% with a period length of 13 monolayers (P = 1.76 nm) and 17 monolayers (P = 2.31

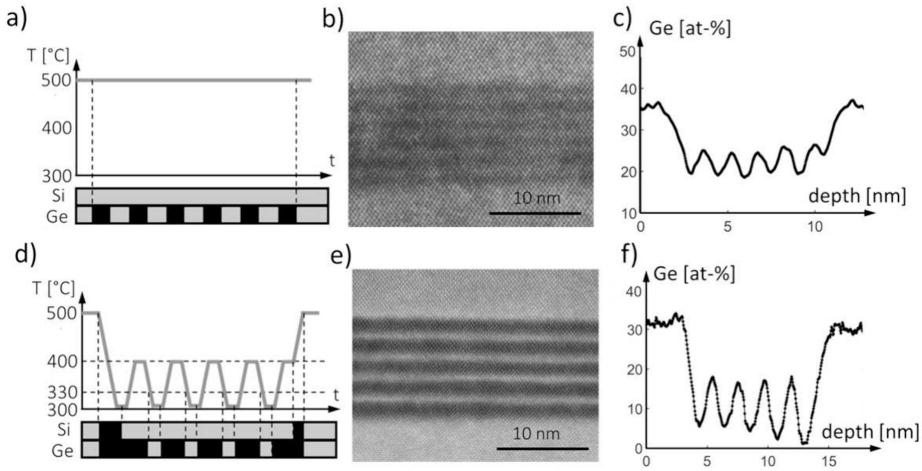

Figure 3. Comparison of two heterostructures grown at constant temperature (a−c) and oscillation growth temperature (d−f), respectively. (a) and (d) show the nominal growth temperature over time together with the Si and Ge shutter configurations where black indicates a closed shutter, with the Si and Ge source kept at the same rate as for the barrier growth. (b, e) Atomic-resolution ADF-STEM images of the heterostructures and (c, f) the Ge concentration along the heterostructure.

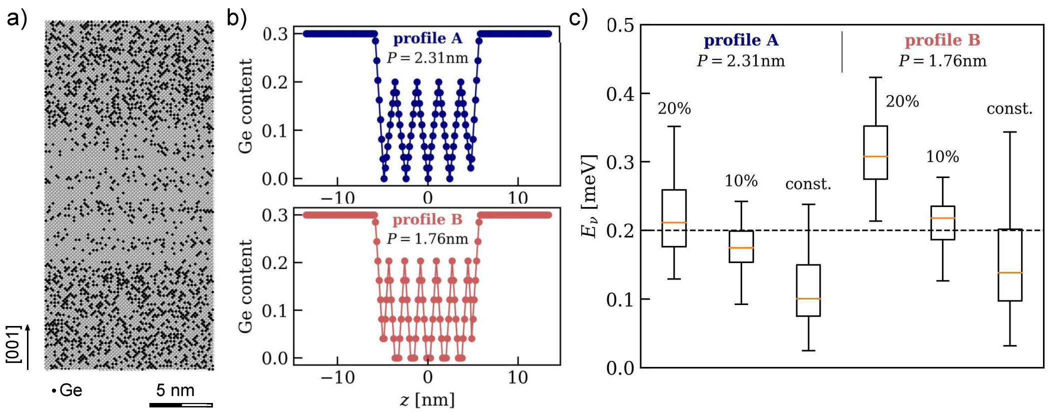

Figure 4. TB model and valley splitting results. (a) Side view of the simulation cell consisting of 230 000 atoms, where the atoms in black represent Ge. (b) Investigated Ge profiles. The length of one oscillation period is given by P. The profile in the top panel is inspired by the Ge profiles in this work. The lower panel shows a Ge profile with a Ge oscillation with wave vector $q = 3.5\ \mathrm{nm}^{-1}$. (c) Results for valley splittings obtained by sp3d5s* TB calculations for the profiles shown in (b) at an electric field of $E_z = 5$ mV/nm. For each Ge profile, the valley splitting of 50 configurations of Ge atoms was calculated and the median values are given by orange lines; the boxes represent the 25−75 percentile ranges, and the whiskers show the full range of data points. Values are given for peak heights of $\hat{n}_{\mathrm{Ge}} = 20\%$, $\hat{n}_{\mathrm{Ge}} = 10\%$ and for constant Ge distributions in the well with the same total amount of Ge as obtained for $\hat{n}_{\mathrm{Ge}} = 20\%$.

nm) were considered, as depicted in Figure 4b. This corresponds to five and four Ge peaks in a 10 nm Si QW layer, respectively.

A constant unmodulated Ge profile (random distribution) in the quantum well layer enhances valley splitting compared with a pure Si one. Hence, the theoretical valley splittings E_ν of the simulated WQWs are compared to QWs containing an equivalent amount of Ge but with a constant concentration profile in Figure 4c. The dashed line in this plot marks E_ν = 200 μeV. This value is large enough to provide a stable platform to host leakage-free electron spin qubit systems, where $E_\nu < 100\ \mu$eV is considered critical for qubit operation.[29] Hence, we utilize 200 μeV as a benchmark. Furthermore, 200 μeV seems to be a rather large value that cannot be reached reliably with clean Si QWs or uncorrelated Ge concentrations in the wells given the data reported in the literature.[29−33]

Profile A in Figure 4b shows a Ge profile that closely resembles the MBE-grown WQW heterostructure presented in Figure 3e, without rounded-off Ge concentration peaks and consequently slightly lower maximal concentration slopes (22%/nm).

As shown in Figure 4c, the theoretical median value for the valley splitting is just above the benchmark value of 200 μeV. This value decreases with decreasing height of the Ge peaks $\hat{n}_{\mathrm{Ge}}$. The oscillating Ge concentration has a significant effect as indicated by the enhancement with respect to wells in which the same amount of Ge is evenly distributed (Ge const.). The median values for E_ν as well as the spreads (indicated by the boxes in Figure 4c) depend on the in-plane size of the simulation cell. Although the median values are well converged for this $13.2 \times 13.2\ \mathrm{nm}^2$ supercell (as shown in the Supporting Information), the actual distributions of E_ν in a quantum device are determined by the lateral extend of the quantum dot. Larger dots will show smaller spreads as a result of self-averaging over the atomic fluctuations in the nanostructure.

Profile B also closely corresponds to the grown WQW heterostructure and could be realized upon further optimization of the herein-proposed growth techniques but is yet to be achieved experimentally. The Ge concentration profile consists of sharp Ge peaks with a maximum concentration slope of 30%/nm and without any intermediate plateaus. This profile shows consequently a shorter period length of $P = 1.76$ nm, which corresponds to a wave vector $q = 2\pi/P = 3.5$ nm^{-1} enabling scattering across the Brillouin zone.[12]

With this profile and $\hat{n}_{Ge} = 20\%$, we anticipate valley splittings reliably above 200 μeV for all realizations as gate-defined quantum dots are typically larger than the considered simulation cell which would decrease the variability in E_ν. Furthermore, a median value as large as $E_\nu = 310$ μeV can be expected for devices based on profile B.

Modifications to Ge oscillations in the WQW, such as spike-like peaks and more trapezoidal-like oscillations, as well as residual Ge concentration in the valleys, were investigated (see Supporting Information). In particular, the calculated valley splitting displays only minor sensitivity to rounding off the sharp peaks of the triangular Ge concentration profiles seen in Figure 4b. We explain this with the Fourier transform of the Ge profile being relatively broad and has finite components in both the 1.8 and 0.32 nm peaks. This explains as well why the choice of the exact value of the oscillation wavelength does not affect the valley splitting a lot.

We interpret this as evidence that the WQW approach is quite robust in enhancing the E_ν, independent of the exact Ge profile. Furthermore, it is important to note that *all investigated WQWs exhibit an increased* E_ν value compared to the equivalent constant Ge distribution.

In summary, we were able to demonstrate a method to suppress Ge segregation during MBE growth of WQW Si/SiGe heterostructure with nanoscale Ge concentration oscillations on the order of 1.7−2.3 nm in the quantum well to enhance valley splitting. This involves an oscillating growth temperature where the growth of interfaces below a certain temperature is required, namely, 300 and 330 °C for Si on SiGe and SiGe on Si, respectively. An elevated intermediate growth temperature of 400 °C ensured smooth surfaces. STEM and APT revealed Ge concentration oscillations with the necessary short period length and concentration slopes of Ge 30%/nm. Tight-binding simulations suggest an average valley splitting of the grown WQW heterostructures of 210 μeV and heterostructure design with values up to 310 μeV, which is well above comparable distributions of Ge with a constant Ge concentration in the QW. Hence, we show that with MBE it is possible to achieve sufficient modulation of the Ge concentration to significantly enhance valley splitting. Therefore, wiggle quantum wells might constitute a promising approach to enhance the performance of Si-based electronic qubits.

■ ASSOCIATED CONTENT

Supporting Information

The Supporting Information is available free of charge at https://pubs.acs.org/doi/10.1021/acs.nanolett.4c05326.

Experimental details on growth of Si/SiGe heterostructures by MBE, including substrate preparation, MBE growth conditions, and in situ annealing; materials characterization using STEM sample preparation and imaging, and APT sample preparation and analysis for concentration profiling; tight-binding simulations of valley splitting based on Ge concentration profiles in the quantum well; complementary experiments on growth by molecular beam epitaxy, details of test structures, Ge oscillation growth parameters, and TEM analysis of Ge segregation; materials characterization using AFM, XRD, STEM, and APT data showcasing heterostructure surface roughness, strain, and composition; simulation robustness from impact of periodic Ge profiles on valley splitting, including imperfections and periodicity robustness; convergence study involving analysis of lateral supercell size effects on valley splitting and alloy disorder influence (PDF)

■ AUTHOR INFORMATION

Corresponding Author

Kevin-P. Gradwohl − *Leibniz-Institut für Kristallzüchtung, 12489 Berlin, Germany;* orcid.org/0000-0003-1841-0289; Phone: +49 (0)30 6392 3021; Email: kevin-peter.gradwohl@ikz-berlin.de; Fax: +49 (0)30 6392 3003

Authors

Lukas Cvitkovich − *Institute for Microelectronics, Technische Universität Wien, 1040 Vienna, Austria*

Chen-Hsun Lu − *Leibniz-Institut für Kristallzüchtung, 12489 Berlin, Germany*

Sebastian Koelling − *École Polytechnique de Montréal, Montréal H3T 1J4 Québec, Canada*

Maximilian Oezkent − *Leibniz-Institut für Kristallzüchtung, 12489 Berlin, Germany;* orcid.org/0000-0001-6435-2599

Yujia Liu − *Leibniz-Institut für Kristallzüchtung, 12489 Berlin, Germany*

Dominic Waldhör − *Institute for Microelectronics, Technische Universität Wien, 1040 Vienna, Austria*

Tibor Grasser − *Institute for Microelectronics, Technische Universität Wien, 1040 Vienna, Austria;* orcid.org/0000-0001-6536-2238

Yann-Michel Niquet − *Université Grenoble Alpes, CEA, IRIG-MEM-L Sim, F-38000 Grenoble, France;* orcid.org/0000-0002-1846-1396

Martin Albrecht − *Leibniz-Institut für Kristallzüchtung, 12489 Berlin, Germany*

Carsten Richter − *Leibniz-Institut für Kristallzüchtung, 12489 Berlin, Germany;* orcid.org/0000-0002-4230-215X

Oussama Moutanabbir − *École Polytechnique de Montréal, Montréal H3T 1J4 Québec, Canada;* orcid.org/0000-0002-0721-3696

Jens Martin − *Leibniz-Institut für Kristallzüchtung, 12489 Berlin, Germany*

Complete contact information is available at: https://pubs.acs.org/10.1021/acs.nanolett.4c05326

Notes

The authors declare no competing financial interest.

■ ACKNOWLEDGMENTS

The authors acknowledge the financial support by the Federal Ministry of Education and Research (BMBF) of Germany in the project QUASAR (Project 13N15659) and the Leibniz Association in the project SiGe Quant (Project K124/2018). This project was funded by the European Union's Horizon 2020 research and innovation program under Grant Agreement 871813, within the framework of the project Modeling Unconventional Nanoscaled DeviceFABrication (MUND-

FAB). Furthermore, funding from the European Research Council (ERC) under grant agreement no. 101055379 is gratefully acknowledged. We also acknowledge the support from the Vienna Scientific Cluster for providing resources on the Austrian high-performance clusters VSC4 and VSC5. O.M. acknowledges support from NSERC Canada (Discovery Grants, Alliance International Quantum, and CQS2Q Consortium), Canada Research Chairs, Canada Foundation for Innovation, Mitacs, PRIMA Québec, Defence Canada (Innovation for Defence Excellence and Security, IDEaS), the European Union's Horizon Europe research and innovation program under Grant Agreement 101070700 (MIRAQLS), the U.S. Army Research Office Grant W911NF-22-1-0277, and the Air Force Office of Scientific and Research Grant FA9550-23-1-0763.

REFERENCES

(1) Evans, P.; Savage, D.; Prance, J.; Simmons, C.; Lagally, M.; Coppersmith, S.; Eriksson, M.; Schülli, T. Nanoscale Distortions of Si Quantum Wells in Si/SiGe Quantum-Electronic Heterostructures. *Adv. Mater.* **2012**, *24*, 5217−5221.

(2) Yoneda, J.; Takeda, K.; Otsuka, T.; Nakajima, T.; Delbecq, M. R.; Allison, G.; Honda, T.; Kodera, T.; Oda, S.; Hoshi, Y.; et al. A quantum-dot spin qubit with coherence limited by charge noise and fidelity higher than 99.9%. *Nat. Nanotechnol.* **2018**, *13*, 102−106.

(3) Xue, X.; Russ, M.; Samkharadze, N.; Undseth, B.; Sammak, A.; Scappucci, G.; Vandersypen, L. M. Quantum logic with spin qubits crossing the surface code threshold. *Nature* **2022**, *601*, 343−347.

(4) Langrock, V.; Krzywda, J. A.; Focke, N.; Seidler, I.; Schreiber, L. R.; Cywiński, Ł. Blueprint of a scalable spin qubit shuttle device for coherent mid-range qubit transfer in disordered Si/SiGe/SiO 2. *PRX Quantum* **2023**, *4*, 020305.

(5) Degli Esposti, D.; Stehouwer, L. E.; Gül, Ö.; Samkharadze, N.; Déprez, C.; Meyer, M.; Meijer, I. N.; Tryputen, L.; Karwal, S.; Botifoll, M.; et al. Low disorder and high valley splitting in silicon. *npj Quantum Inf.* **2024**, *10*, 32.

(6) Hollmann, A.; Struck, T.; Langrock, V.; Schmidbauer, A.; Schauer, F.; Leonhardt, T.; Sawano, K.; Riemann, H.; Abrosimov, N. V.; Bougeard, D.; et al. Large, tunable valley splitting and single-spin relaxation mechanisms in a Si/Si x Ge 1- x quantum dot. *Physical review applied* **2020**, *13*, 034068.

(7) Volmer, M.; Struck, T.; Sala, A.; Chen, B.; Oberländer, M.; Offermann, T.; Xue, R.; Visser, L.; Tu, J.-S.; Trellenkamp, S.; et al. Mapping of valley splitting by conveyor-mode spin-coherent electron shuttling. *npj Quantum Inf.* **2024**, *10*, 61.

(8) Künne, M.; Willmes, A.; Oberländer, M.; Gorjaew, C.; Teske, J. D.; Bhardwaj, H.; Beer, M.; Kammerloher, E.; Otten, R.; Seidler, I.; et al. The SpinBus architecture for scaling spin qubits with electron shuttling. *Nat. Commun.* **2024**, *15*, 4977.

(9) Zwerver, A.; Krähenmann, T.; Watson, T.; Lampert, L.; George, H. C.; Pillarisetty, R.; Bojarski, S.; Amin, P.; Amitonov, S.; Boter, J.; et al. Qubits made by advanced semiconductor manufacturing. *Nature Electronics* **2022**, *5*, 184−190.

(10) Paquelet Wuetz, B.; Losert, M. P.; Koelling, S.; Stehouwer, L. E.; Zwerver, A.-M. J.; Philips, S. G.; Mądzik, M. T.; Xue, X.; Zheng, G.; Lodari, M.; et al. Atomic fluctuations lifting the energy degeneracy in Si/SiGe quantum dots. *Nat. Commun.* **2022**, *13*, 7730.

(11) McJunkin, T.; MacQuarrie, E.; Tom, L.; Neyens, S.; Dodson, J.; Thorgrimsson, B.; Corrigan, J.; Ercan, H. E.; Savage, D.; Lagally, M.; et al. Valley splittings in Si/SiGe quantum dots with a germanium spike in the silicon well. *Phys. Rev. B* **2021**, *104*, 085406.

(12) McJunkin, T.; Harpt, B.; Feng, Y.; Losert, M. P.; Rahman, R.; Dodson, J.; Wolfe, M.; Savage, D.; Lagally, M.; Coppersmith, S.; et al. SiGe quantum wells with oscillating Ge concentrations for quantum dot qubits. *Nat. Commun.* **2022**, *13*, 7777.

(13) Woods, B. D.; Soomro, H.; Joseph, E.; Frink, C. C.; Joynt, R.; Eriksson, M.; Friesen, M. Coupling conduction-band valleys in SiGe heterostructures via shear strain and Ge concentration oscillations. *npj Quantum Inf.* **2024**, *10*, 54.

(14) Woods, B. D.; Eriksson, M.; Joynt, R.; Friesen, M. Spin-orbit enhancement in Si/SiGe heterostructures with oscillating Ge concentration. *Phys. Rev. B* **2023**, *107*, 035418.

(15) Dyck, O.; Leonard, D. N.; Edge, L. F.; Jackson, C. A.; Pritchett, E. J.; Deelman, P. W.; Poplawsky, J. D. Accurate quantification of Si/SiGe interface profiles via atom probe tomography. *Adv. Mater. Interfaces* **2017**, *4*, 1700622.

(16) Grützmacher, D.; Sedgwick, T.; Powell, A.; Tejwani, M.; Iyer, S. S.; Cotte, J.; Cardone, F. Ge segregation in SiGe/Si heterostructures and its dependence on deposition technique and growth atmosphere. *Applied physics letters* **1993**, *63*, 2531−2533.

(17) Gravesteijn, D. J.; van De Walle, G. F.; van Gorkum, A. A. Silicon molecular beam epitaxy. *Adv. Mater.* **1991**, *3*, 351−355.

(18) Iyer, S. S.; Patton, G. L.; Stork, J. M.; Meyerson, B. S.; Harame, D. L. Heterojunction bipolar transistors using Si-Ge alloys. *IEEE Trans. Electron Devices* **1989**, *36*, 2043−2064.

(19) Fukatsu, S.; Fujita, K.; Yaguchi, H.; Shiraki, Y.; Ito, R. Self-limitation in the surface segregation of Ge atoms during Si molecular beam epitaxial growth. *Applied physics letters* **1991**, *59*, 2103−2105.

(20) Zalm, P.; Van De Walle, G.; Gravesteijn, D.; Van Gorkum, A. Ge segregation at Si/Si1- x Ge x interfaces grown by molecular beam epitaxy. *Applied physics letters* **1989**, *55*, 2520−2522.

(21) Fukatsu, S.; Usami, N.; Fujita, K.; Yaguchi, H.; Shiraki, Y.; Ito, R. Is low temperature growth the solution to abrupt Si Si1-xGex interface formation? *Journal of crystal growth* **1993**, *127*, 401−405.

(22) Abrosimov, N.; Aref'Ev, D.; Becker, P.; Bettin, H.; Bulanov, A.; Churbanov, M.; Filimonov, S.; Gavva, V.; Godisov, O.; Gusev, A.; et al. A new generation of 99.999% enriched 28Si single crystals for the determination of Avogadro's constant. *Metrologia* **2017**, *54*, 599.

(23) Yamashita, S.; Kikkawa, J.; Yanagisawa, K.; Nagai, T.; Ishizuka, K.; Kimoto, K. Atomic number dependence of Z contrast in scanning transmission electron microscopy. *Sci. Rep.* **2018**, *8*, 12325.

(24) Eberl, K.; Wegscheider, W.; Abstreiter, G. Group IV element (Si, Ge and α-Sn) superlattices—low temperature MBE. *Journal of crystal growth* **1991**, *111*, 882−888.

(25) Eberl, K.; Friess, E.; Wegscheider, W.; Menczigar, U.; Abstreiter, G. Improvement of structural properties of Si/Ge superlattices. *Thin Solid Films* **1989**, *183*, 95−103.

(26) Niquet, Y. M.; Rideau, D.; Tavernier, C.; Jaouen, H.; Blase, X. Onsite matrix elements of the tight-binding Hamiltonian of a strained crystal: Application to silicon, germanium, and their alloys. *Phys. Rev. B* **2009**, *79*, 245201.

(27) Keating, P. N. Effect of Invariance Requirements on the Elastic Strain Energy of Crystals with Application to the Diamond Structure. *Phys. Rev.* **1966**, *145*, 637−645.

(28) Losert, M. P.; Eriksson, M. A.; Joynt, R.; Rahman, R.; Scappucci, G.; Coppersmith, S. N.; Friesen, M. Practical strategies for enhancing the valley splitting in Si/SiGe quantum wells. *Phys. Rev. B* **2023**, *108*, 125405.

(29) Losert, M. P.; Eriksson, M.; Joynt, R.; Rahman, R.; Scappucci, G.; Coppersmith, S. N.; Friesen, M. Practical strategies for enhancing the valley splitting in Si/SiGe quantum wells. *Phys. Rev. B* **2023**, *108*, 125405.

(30) Shi, Z.; Simmons, C. B.; et al. Tunable singlet-triplet splitting in a few-electron Si/SiGe quantum dot. *Appl. Phys. Lett.* **2011**, *99*, 233108.

(31) Kawakami, E.; Scarlino, P.; Ward, D. R.; Braakman, F. R.; Savage, D. E.; Lagally, M. G.; Friesen, M.; Coppersmith, S. N.; Eriksson, M. A.; Vandersypen, L. M. K. Electrical control of a long-lived spin qubit in a Si/SiGe quantum dot. *Nat. Nanotechnol.* **2014**, *9*, 666−670.

(32) Mi, X.; Péterfalvi, C. G.; Burkard, G.; Petta, J. R. High-Resolution Valley Spectroscopy of Si Quantum Dots. *Phys. Rev. Lett.* **2017**, *119*, 176803.

(33) Oh, S. W.; Denisov, A. O.; Chen, P.; Petta, J. R. Cryogen-free scanning gate microscope for the characterization of Si/Si0.7Ge0.3

quantum devices at milli-Kelvin temperatures. *AIP Adv.* **2021**, *11*, 125122.

https://doi.org/10.1021/acs.nanolett.4c05326
Nano Lett. 2025, 25, 4204−4210